

Deep Saturated Free Electron Laser Oscillators and Frozen Spikes

P. L. Ottaviani, S. Pagnutti*

ENEA - Centro Ricerche Bologna, via Martiri di Monte Sole, 4 , IT 40129 Bologna, Italy

G. Dattoli, E. Sabia†

*ENEA - Centro Ricerche Frascati, via E. Fermi,
45, IT 00044 Frascati (Roma), Italy*

V. Petrillo‡

*Universita' degli Studi di Milano, via Celoria 16, IT 20133 Milano, Italy and
INFN - Mi , via Celoria 16, IT 20133 Milano, Italy*

P. Van Der Slot§

*University of Twente, P.O.Box 217,
7500 AE Enschede (The Netherlands)*

S. Biedron and S. Milton¶

Department of Electrical and Computer Engineering Colorado State University (USA)

Abstract

We analyze the behavior of Free Electron Laser (FEL) oscillators operating in the deep saturated regime and point out the formation of sub-peaks of the optical pulse. They are very stable configurations, having a width corresponding to a coherence length. We speculate on the physical mechanisms underlying their growth and attempt an identification with FEL mode locked structures associated with Super Modes. Their impact on the intra-cavity nonlinear harmonic generation is also discussed along with the possibility of exploiting them as cavity out-coupler.

*Electronic address: simonetta.pagnutti@enea.it

†Electronic address: giuseppe.dattoli@enea.it; Electronic address: elio.sabia@enea.it

‡Electronic address: vittoria.petrillo@mi.infn.it

§Electronic address: p.j.m.vanderslot@utwente.nl

¶Electronic address: biedron@anl.gov; Electronic address: milton@engr.colostate.edu

I. INTRODUCTION

In a Free Electron Laser (FEL) oscillator the optical pulses go back and forth inside the cavity and, at the undulator entrance, overlap with fresh electron bunches, reinforcing the relevant intensity, until gain equals the cavity losses[1]. The pivoting parameters of the game are defined below

$$\begin{aligned}\Delta &= N\lambda_s \equiv \textit{Slippage Length} \\ \sigma_z &\equiv \textit{Bunch Length}\end{aligned}\tag{1}$$

with N , λ_s being the number of periods of the undulator and the resonant wavelength, respectively. The physical origin of Δ is associated with the different velocities of electron and radiation packets, determining an advance of the radiation, after an undulator passage, by just a slippage length. For an appropriate quantification of the effects induced by such a longitudinal mismatch the following parameter has been introduced [2]

$$\mu_c = \frac{\Delta}{\sigma_z}\tag{2}$$

which has a manifold role. It provides indeed a measure of the number of longitudinal modes, locked during the interaction and the gain reduction itself induced by the spoiled longitudinal overlapping. To understand the reason why the parameter μ_c is associated with mode locking, we just remind that the longitudinal mode gain of a FEL driven by a short pulse electron beam is linked to the Fourier Transform of the pulse itself [2] and discuss the relevant details in appendix A.

Slippage and mode coupling cannot be considered disentangled and should be viewed within the context of the short pulse oscillator dynamics, also characterized by the lethargy mechanism, due to the slowing down of the optical packet velocity, while interacting with the electrons inside the optical cavity. As a consequence either the gain and the cavity equilibrium power depends on the cavity detuning parameter

$$\theta = \frac{4\delta L}{g_0\Delta}\tag{3}$$

where δL is the cavity mismatch from the ideal length ¹, introduced to compensate the lethargy effect and g_0 is the small signal gain coefficient. The intra-cavity intensity round trip evolution can be reproduced by fairly simple formulae [3], reported below.

$$\begin{aligned}
I_r(\theta, \mu_c) &= I_0 \frac{\{(1 - \eta) [G(\theta, \mu_c) + 1]\}^r}{1 + \frac{I_0}{I_e}(\theta, \mu_c) \{[(1 - \eta) (G(\theta, \mu_c) + 1)]^r - 1\}}, \\
I_e(\theta, \mu_c) &\cong (1 + \sqrt{2}) \left\{ \sqrt{\frac{\theta^*}{\theta}} \exp \left[\frac{1}{2} \left(1 - \frac{\eta}{(1 - \eta) G^*} \frac{\theta^*}{\theta} \right) \right] - 1 \right\} I_s, \\
G(\theta, \mu_c) &= G_M \frac{\theta}{\theta_s} \left[1 - \ln \left(\frac{\theta}{\theta_s} \gamma_c \right) \right], \quad G_M \cong 0.85g_0, \quad \theta_s \cong 0.456, \quad \gamma_c = 1 + \frac{\mu_c}{3}, \\
0 \leq \theta \leq e \frac{\theta_s}{\gamma_c}, \quad G^* &= \frac{G_M}{\gamma_c}, \quad \theta^* = \frac{\theta_s}{\gamma_c}, \quad e \equiv \text{Neper number}
\end{aligned} \tag{4}$$

where r denotes the round trip number, I_0 the initial seed, G the small signal gain, I_s denotes the FEL saturation intensity, I_e the equilibrium intra-cavity intensity and η the cavity losses. The gain dilution due to the slippage and to the finite bunch length is provided by γ_c . It should be noted that eq. (4) yields the intensity intracavity evolution under the assumption of low gain, it can therefore be considered valid only for values of the small signal coefficient not exceeding 0.3. In this approximation the gain function $G(\theta, \mu_c)$ is vanishing at zero cavity detuning, the relevant meaning and limit of validity will be discussed in the following. For a more accurate parametrization, including high gain corrections, the reader is addressed to refs. [3] and for further comments to ref. [4].

The previous formulae provide a fairly reasonable description of the FEL oscillator dynamics in terms of laser intensity evolution, but do not provide any information on the pulse growth and shaping, occurring during the evolution and on the relevant dependence on the various parameters.

¹ By ideal cavity length we mean that corresponding to a round trip allowing the overlapping between two successive bunches of electron and photons.

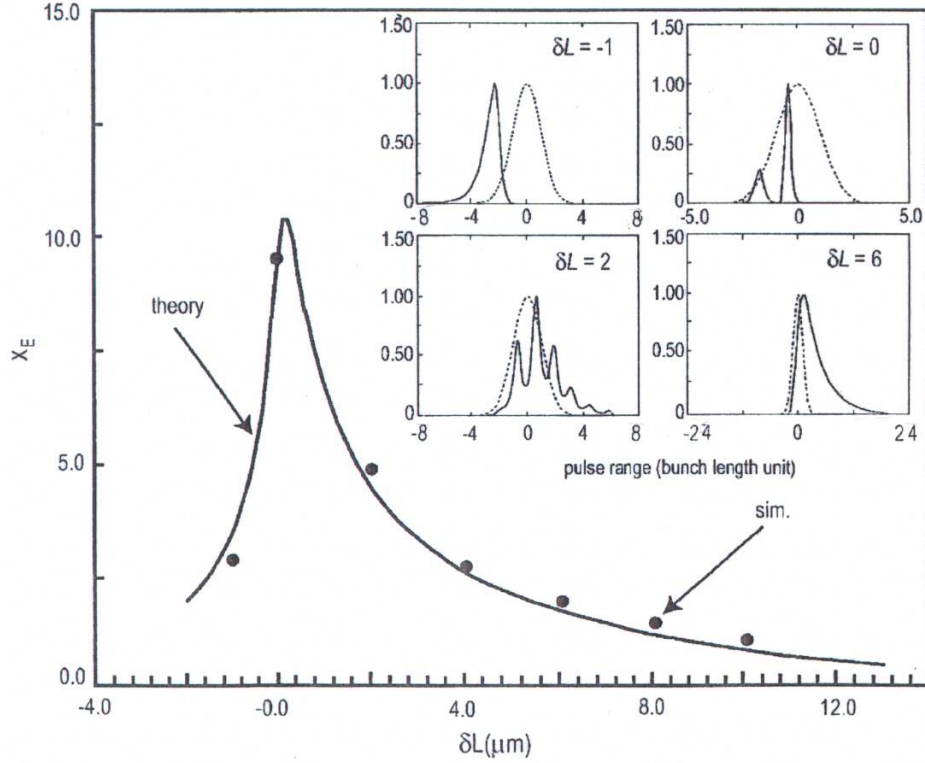


Figure 1: Oscillator FEL intra-cavity equilibrium power: analytical (continuous line), numerical (dots) and pulse shape (continuous line) for different cavity detunings (electron pulse dash line). ($g = 2.0$, $\mu_c = 1$, $\eta = 0.06$. In this case the large gain value allows the growth of the laser field even for negative values of θ)

In Fig.1 a largely well-known feature is reported regarding the dependence of the optical pulse shape on the cavity mismatch itself, the occurrence of different peaks has also been recognized as a manifestation of the locking of different Super Mode structures [2]. It should be noted that the concept of Super Mode has been used improperly. According to the original formulation they are low gain small signal self reproducing collection of longitudinal modes. They are characterized by vanishing gain at zero cavity detuning. The fact that they have no gain at zero cavity desynchronization does not mean that FEL oscillators cannot lase in this configuration, it only means that for $\theta = 0$ there are not stationary modes of S. M. type allowed by the FEL dynamics. In any case these modes provide a suitable basis allowing the FEL pulse expansion and eq. (4) provides a reasonable approximation to describe the intensity FEL oscillator evolution in the pulsed regime. Subsequent elaboration

(either numerical and analytical) [3, 5] have clarified the role of the high gain contributions, as we will further discuss in the following.

The FEL oscillator pulse dynamics becomes more intrigued with the system undergoing deeper and deeper saturated regime [6]. One of the most interesting phenomenon occurring at this level is the emergence of a comb structure inside the optical pulse itself, consisting of a series of sub-pulses with a length comparable to a coherence length.

In this paper we speculate on the physical mechanisms underlying the emergence of these spikes and discuss the feedback on the intra-cavity harmonic generation. In the following we will exploit the code PROMETEO to analyze the evolution of the FEL oscillator dynamics from small signal to deep saturated regime. The results of the code, which does not contain three dimensional effects, will be compared with those from GENESIS, which brings further and deeper insight by allowing the possibility of understanding the interplay between transverse and longitudinal modes.

II. DEEP SATURATION AND OPTICAL PULSE OSCILLATOR DYNAMICS

In Fig.2 we report a series of snap-shots describing the growth of an optical pulse at different round trips, inside the optical cavity set at zero detuning. The relevant dynamics is, at the beginning, fairly transparent; the pulses grow in the form of a homogeneous and almost Gaussian distribution, which over the round trips, tend to spread over all the electron bunch length. One of the consequence of the lethargy mechanism is an asymmetry, getting more pronounced with increasing saturation and characterized by a sharp front edge.

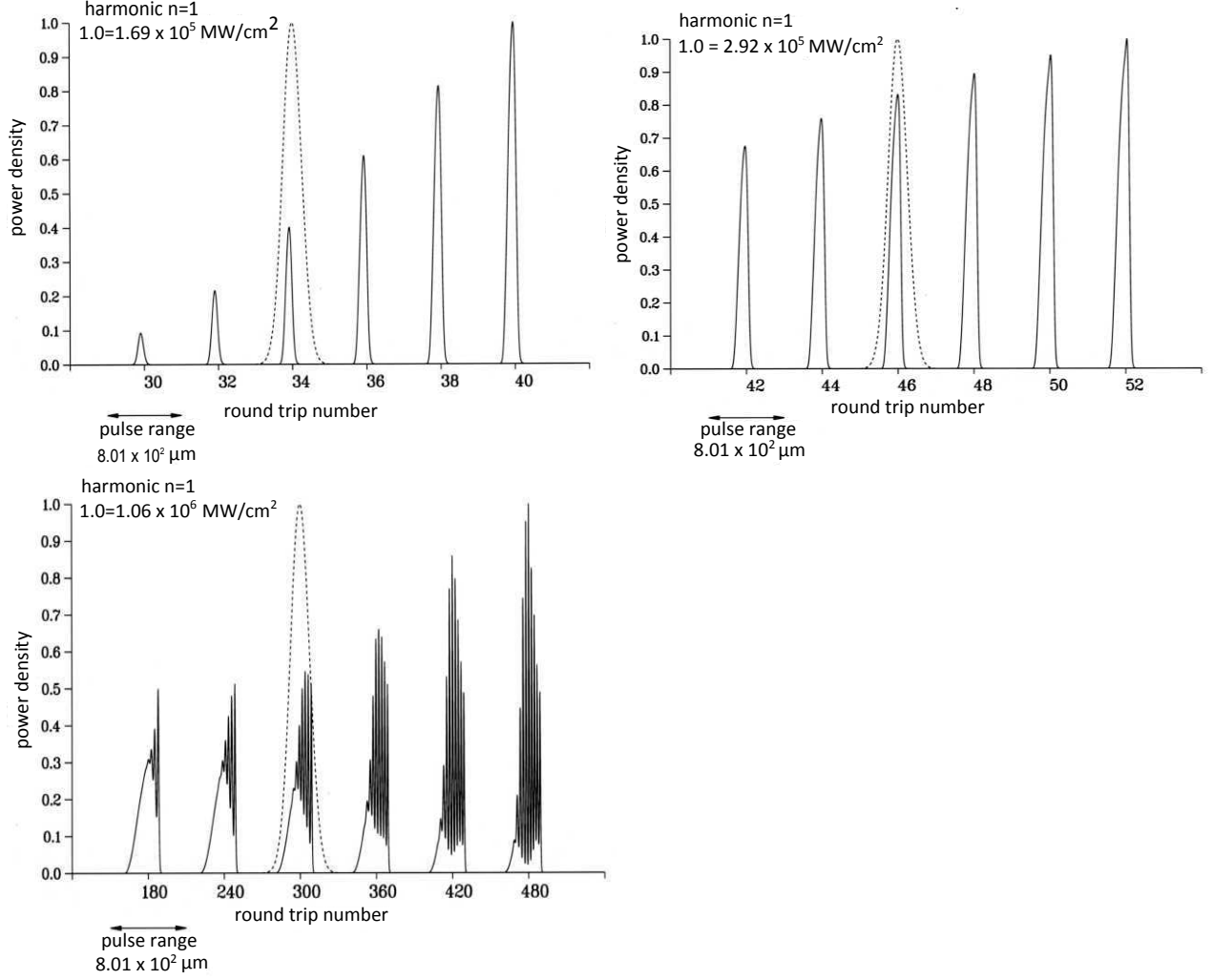


Figure 2: Evolution of the optical packet distribution at different round trip; simulation parameters are given below $E = 155.3 \text{ Mev}$, $J = 2.68 \cdot 10^8 \frac{\text{A}}{\text{m}^2}$, $\rho = 2.33 \cdot 10^{-3}$, $\sigma_\varepsilon = 10^{-4}$, $\sigma_z = 100 \mu\text{m}$, $g_0 = 1$, $\eta = 0.06$, *number of periods* $N = 77$, $\lambda_s = 500.33 \text{ nm}$, $\Delta = 38.5 \mu\text{m}$, $l_c = 9.78 \mu\text{m}$

However in the small signal regime and at moderated saturation levels, the laser-pulse shape is not far from a Gaussian with a bunch length given by

$$\sigma_b \cong \frac{1}{2} \sqrt{\Delta \sigma_z} \quad (5)$$

While the saturation increases, the bunch acquires a modulation, starting from the front part and covering progressively the entire electron bunch, as shown in Fig.3, where we have picked out the optical pulse distribution at the round trip number 480. For the chosen parameters of the simulation (cavity length and macro-pulse e-beam structure) this number

of round trip corresponds to tens of microseconds of time duration. The observation of such a comb structure requires therefore quite a long operation time.

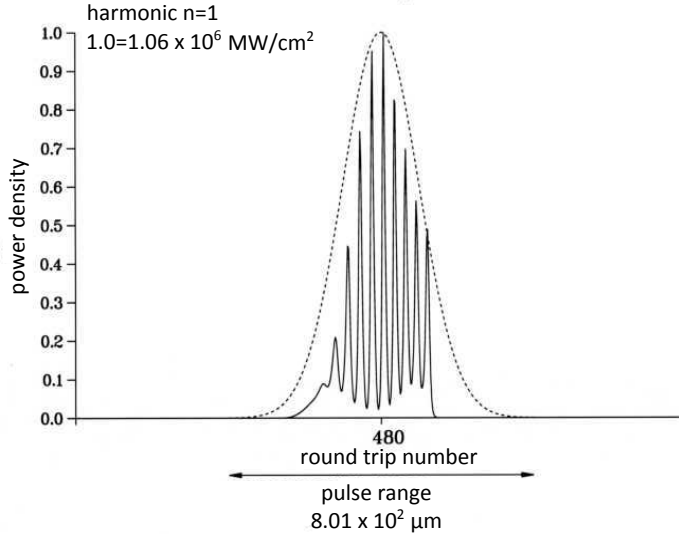


Figure 3: Optical packet “equilibrium” configuration; simulation parameters as in Fig.2

As already remarked, the slippage length is a measure of the maximum amount of the optical packet slippage over the electrons, due to the different velocities. The introduction of such a quantity is however based on purely kinematical argument, the motion of the optical pulse inside the electrons cannot be indeed merely viewed as a slippage. The electrons move indeed in a dispersive medium. The interaction itself should be characterized by an index of refraction, which in turn provides the already quoted lethargy mechanism. The FEL refractive index is a quantity of paramount importance, which is easily specified in terms of analytical formulae in the small signal regime. When saturation occurs, the gain (which is essentially linked to the real part of the refractive index) is decreased by the laser intracavity power itself and the same holds for the imaginary part. The concomitance of these mechanisms allows the formation of substructures growing around the coherence length. We have analyzed the peak formation using different values of the parameters entering the definition of the FEL evolution process. We have therefore examined cases with different gain coefficients and bunch length and we have found that the number of spikes formed in deep saturation does not depend on the number of undulator periods and seems to be associated with the coherence length of the process itself, we have therefore made the following ansatz

(the sub-index S stays for "Spike")

$$n_S \cong \frac{\sigma_z}{\sigma_S}, \quad \sigma_S \cong l_c = \frac{\lambda_s}{4\pi\rho\sqrt{3}} \quad (6)$$

where l_c is the coherence length [6] (λ_s and ρ are the wavelength and Pierce parameter, respectively) (for further comments see Appendix).

In the description of the spike formation phenomenology, we have deliberately used a language and a notation more appropriate to SASE than to oscillator FEL devices, the peaks we are describing resemble the spikes of the high gain regime; they become locked in phase by the operating conditions in the optical cavity. Such an identification is not new, either from the theoretical and experimental point view [7] and we will further comment on this point in the concluding section of the paper.

In Tab.I we have reported the power density of the peaks of the pulse shown in Fig. 3 (numerated from the left to the right).

Before going further let us remind that, along with the fundamental, higher order harmonics are generated inside the optical cavity. In Fig.4 we have reported the power of the first harmonic stored in the cavity and the power radiated (not stored) at higher harmonics during each round trip for the case $g_0 = 1.5$.

As it is well known, the non-linear harmonic generation is a by-product of the FEL process itself and is due to the bunching mechanism induced by the fundamental harmonics. The maximum of the harmonic emission occurs before the first harmonic reaches the stationary condition. In the successive round trips the harmonic power drops down owing to the large energy spread induced by the FEL interaction itself.

Peak number	Power density ($\frac{MW}{cm^2}$)
1	9.32×10^4
2	2.21×10^5
3	4.71×10^5
4	7.85×10^5
5	1.01×10^6
6	1.06×10^6
7	8.71×10^5
8	7.37×10^5
9	5.95×10^5
10	5.17×10^5

Table I: Peak number and relevant power at the 480th round trip.

An interesting feature we observe in deep saturation is the presence of a reinforcement of the power emitted at higher harmonics. This effect should be understood as an increase in the efficiency of the harmonic generation associated with the intrinsic super-radiant nature of the emission process. The spiking distribution of the radiation explores fresh region of the electron bunch ensuring a more copious emission of radiation. An idea of the interplay between the pulse distribution of the harmonic and the side band occurring at the fundamental is provided in Figs. 5 and 6, where we have reported both the pulse harmonic evolution at different round trip and the “stationary” distribution

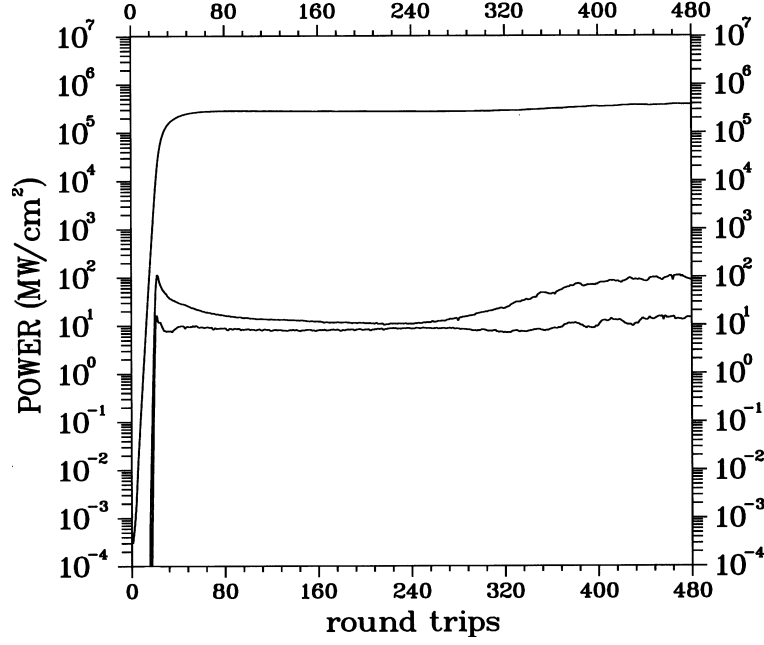


Figure 4: Fundamental and higher order harmonic (3-rd and 5-th) power vs. round trip number (the 1-st harmonic is stored, the other are just radiated coherently at each round trip). Simulation parameters: (The number of n_S calculated with eq. (6) for this specific case is 9) $E = 155.3 \text{ Mev}$, $J = 4.01 \cdot 10^8 \frac{\text{A}}{\text{m}^2}$, $\rho = 2.67 \cdot 10^{-3}$, $\sigma_\varepsilon = 10^{-4}$ (*relative energy spread*), $\sigma_z = 100 \mu\text{m}$, $\eta = 0.06$, *Number of undulator periods* $N = 77$, $\lambda_s = 500.24 \text{ nm}$, $l_c = 8.66 \mu\text{m}$

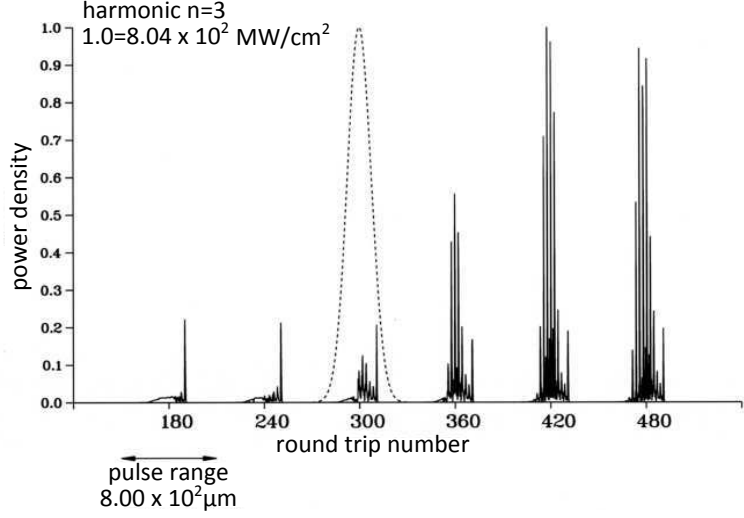


Figure 5: Pulse distribution of the third harmonic at different round trips, same parameters as in Fig.4

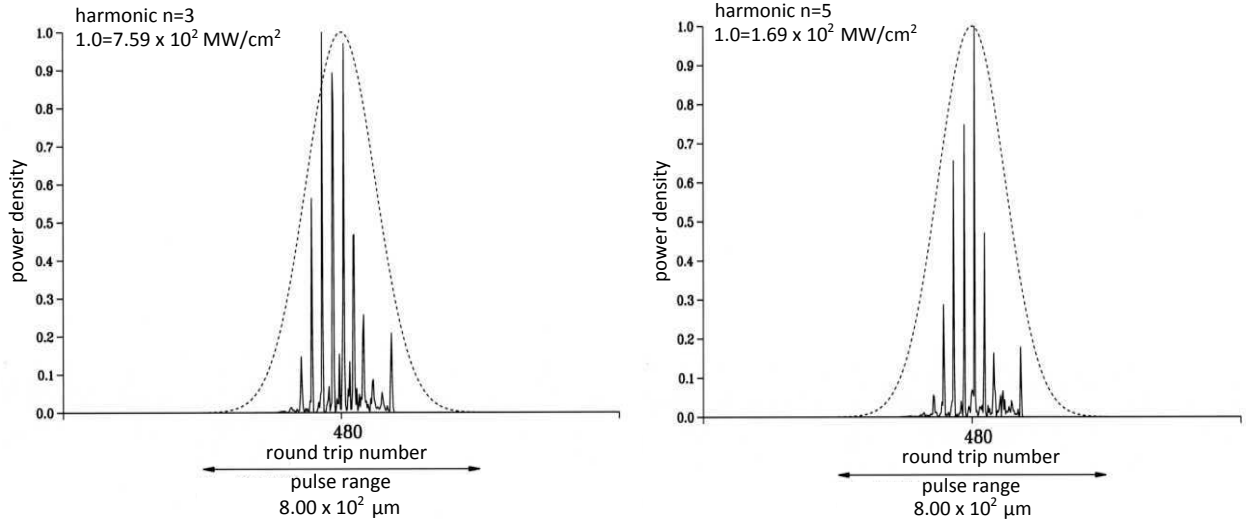


Figure 6: Third and fifth harmonic distribution at 480-th round trip, same parameters as in Fig.4

The dynamics of the harmonic pulses, along with the relevant side band, is quite transparent. Initially a more substantive harmonic generation occurs on the trailing part of the beam where the bunching is stronger, when the peaks shift towards the rear edge of the packet, the side bands become increasingly larger in that region.

What we have described so far is the crude “phenomenology”, which shows that the generation of stable sub-pulses with a length of the order of a coherence length occurs in

deeply saturated FEL oscillators. The results we have so far obtained confirm the formation of side bands at zero cavity detuning in deeply saturated conditions [4, 7] The existence of spikes in high gain FEL oscillators at zero desynchronism has already been discussed in the past either theoretically and experimentally in refs. [4, 6] where the possible link with the spikes characterizing the high gain behaviour has also been pointed out. We have in addition pointed out that the pulses associated with the higher order harmonics exhibit an analogous side band structure. In the forthcoming section we will draw further consequences also of practical nature.

III. FEL DEEP SATURATED REGIME AND OUTPUT COUPLING

We have stressed that the harmonic radiation is not stored in the optical cavity but it represents just the power radiated on higher harmonics at each round trip. The question arises therefore of how the associated amount of power can be coupled out. Since in our example we have considered a FEL operating in the visible (around 500 nm), the third and fifth harmonic wavelength are at 165 and 100 nm, and therefore much of the radiation could be absorbed by the mirrors. This drawback becomes more significant at shorter wavelength.

A problem of practical interest is therefore that of coupling the harmonic power outside. A possibility is offered by the use of an external radiator, provided by an undulator with the same characteristics of the intracavity magnet. The e-b extracted from the cavity and injected inside the radiator produces the effects shown in Fig. 7. When the oscillator operates in the deep saturated regime, the electrons in the second undulator radiate an almost exact replica of the of the intracavity first harmonic field intensity (albeit the associated pulse slips over the electrons and acquires a more asymmetric shape of its intracavity counterpart). The corresponding third harmonic power grows very nicely and may reach significant power levels. It is however remarkable that the level of laser power is so strong that it impresses complete memory of its comb structure on the fresh electron bunch, which is bunched in such a way to restore, in a kind of eco, the harmonic generation inside the cavity. If this effect holds in an actual experimental configuration, it could be exploited as an out-coupler mechanism, thus providing an extremely useful extraction tool, if e.g. the cavity optics absorb the radiation emitted at higher harmonics.

A different situation occurs in the case in which the external undulator is adjusted at the

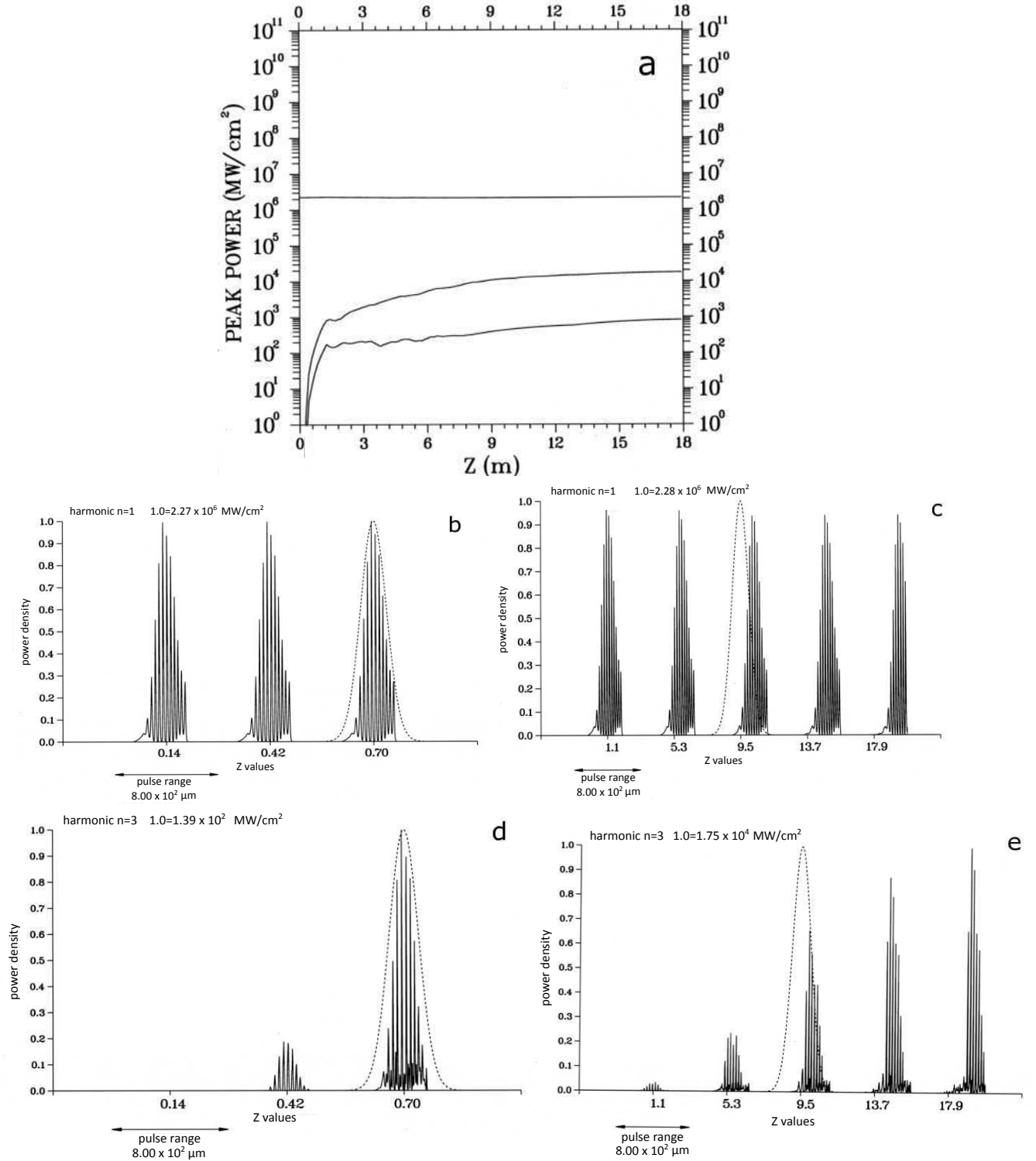


Figure 7: Radiation emitted by the electrons in the external undulator: a) intensity growth for the first harmonic (which remains constant) and third and fifth, the power level of the harmonics reaches the maximum with a relatively short undulator; b) fundamental harmonic in the first 0.7 m of the undulator; c) same as b up to 18 m; d) third harmonic in the first 0.7 m of the undulator; e) same as d up to 18 m.

third harmonic of the first. In this case we obtain what is indicated in Figs. 8. The radiation is initially extracted from the intra-cavity undulator in quite an unperturbed form and is conserved over a small distance (of the order of one meter) inside the external undulator. After this lethargic phase, the system rearranges its phase space to adjust itself into a configuration which has lost memory of the phase locking inside the oscillator and allows intensity growth, with the unavoidable destruction of the comb structure.

It is evident that the phase locking acquired in the cavity cannot be maintained outside, if the external undulator has different characteristics from that driving the oscillator.

IV. FINAL COMMENTS

We have already guessed that the sub-peaks appearing in the deep saturated oscillator regime could be viewed as the stable version of the spikes occurring in the SASE operation.

The intensity random fluctuations affecting the case of the latter regime are not present in the oscillator configuration, because they are locked in phase by the interplay of the intensity growth and by the coupling of the longitudinal modes due to the electron bunch itself.

The mechanism underlying the longitudinal mode coupling in pulsed FEL oscillators has been discussed in the past and it was shown that FEL multimode gain depends on the Fourier transform of the electron beam itself [8]. Such a phase locking provides the first step towards the comb structure in deep saturated regime.

The relevant dynamics can however be explained using as paradigmatic well known mechanisms widely studied in conventional laser Physics.

We note first that the intra-cavity evolution in the small signal regime and for small cavity losses $\eta \ll 1$ is dominated by a mechanism analogous to the active mode locking by loss modulation [9]. In the present case the modulation occurs through the bunch current shape. The relevant master equation for the complex field amplitude A can be written as [2]

$$T_R \frac{\partial}{\partial T} A = \left[(G_1 - \eta) + \mu_c (G_2 - \theta) \frac{\partial}{\partial \tau} + \frac{1}{2} G_3 \frac{\partial^2}{\partial \tau^2} - \frac{1}{2} G_1 \tau^2 \right] A$$

$$\tau = \frac{z}{\sigma_z}, \quad T_R = 2 \frac{L_c}{c}, \quad L_c \equiv \text{Cavity length} \quad (7)$$

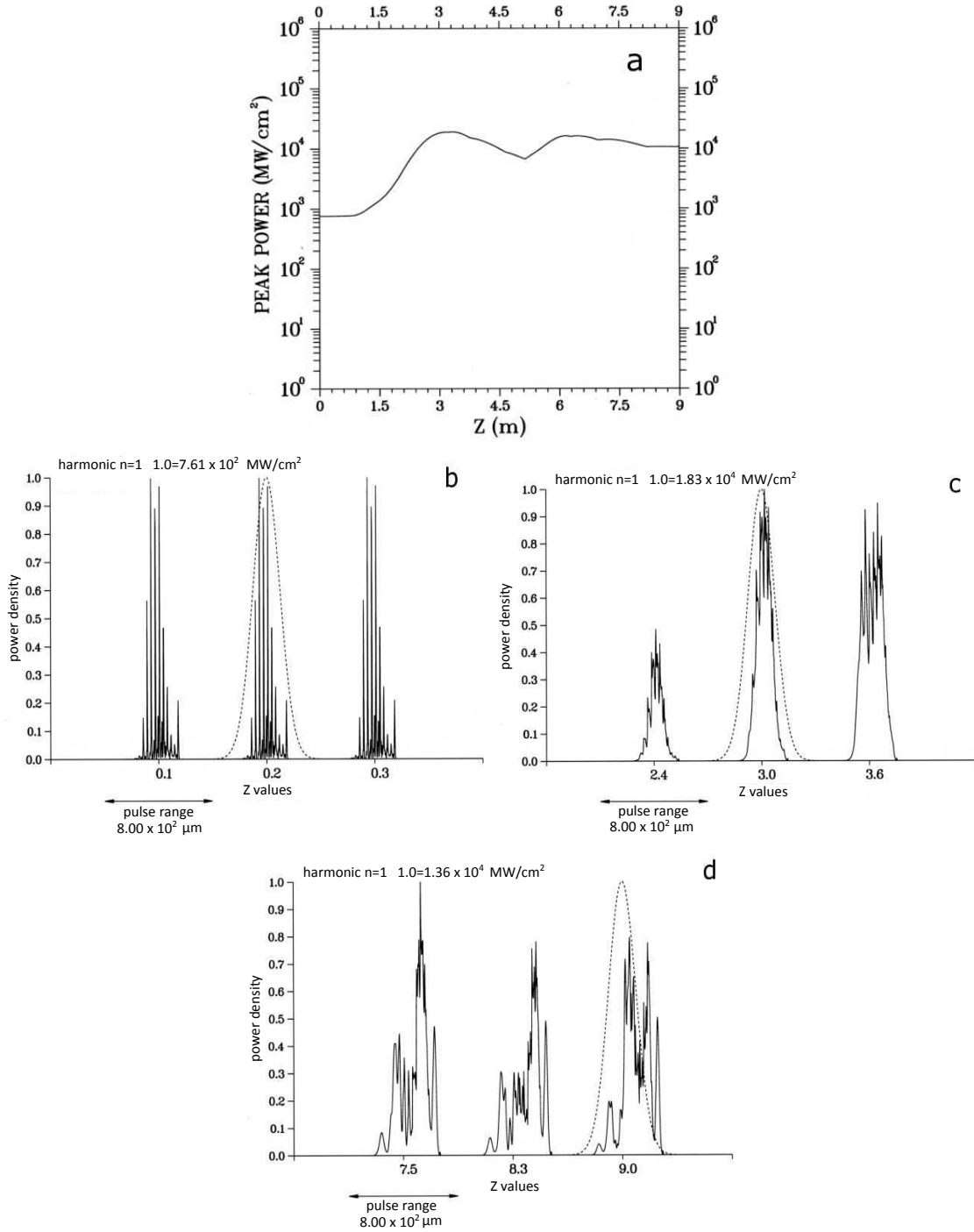


Figure 8: a) Harmonic power evolution outside the cavity; b) optical pulse shape in the first undulator section (30 cm); c) Same as b) further along the undulator; d) Same as b) along the last part of the undulator .

where τ is the longitudinal coordinate, normalized to the bunch rms length, $G_{1,2,3}$ are complex quantities associated to the FEL gain and η and θ have been defined previously. Furthermore, the equation has been obtained by approximating the finite difference equation, in terms of round trip number, with a first order differential equation in the time T defined as $T \cong rT_R$.

Eq. (7) holds for optical pulses around the centre of the electron bunch and is fully equivalent to its counterpart in conventional laser physics. There are several reasons why we have reported eq. (7), which holds in the case of small signal low gain regime. Apart from the fact that there is a one to one mapping with similar equations accounting for active mode locking in conventional lasers, we note that from the mathematical point of view, eq. (7) is a master equation with a quadratic potential. Its stationary solutions are provided by Hermite-Gauss modes, and provide the Super Modes for the problem under study [10, 11], namely small slippage compared to the electron bunch length. The gain of each eigenmode is not zero at 0 cavity detuning (the maximum gain is given by the condition $\theta = G_3$). Equation (7) can be used to model the saturation provided that the gain terms be replaced by the corresponding gain saturated forms (see Appendix for further details). It should be stressed that eq. (7) assumes that the mode growth occurs around the maximum of the electron bunch distribution and indeed the quadratic terms in τ^2 is due to an expansion of the current profile up to the lowest order in the longitudinal coordinate. This is also compatible with the assumption that the slippage is small compared to the bunch length and, therefore, that the mode longitudinal extension cover a limited portion of the electron bunch. The small slippage approximation allows the possibility of studying the field evolution around the center of the electron packet. Other SM like forms may grow in correspondence of other positions inside the e-bunch, after saturation around the maximum of the current has occurred.

The fundamental mode, namely that corresponding to the lowest order eigenmode of eq. (7), has the largest gain and is the more likely to reach saturation, it has a gaussian shape, having the width reported in eq. (6) (See Appendix).

We must however emphasize that during the evolution the optical pulse tends to move towards the front end of the electron bunch, this determines a faster saturation of the “active-medium” represented by this portion of the bunch. It should now be kept in mind that the lowest order SM is that reaching the saturation, while the others die, before that the system

approaches the equilibrium. The survival of only one mode ensures the stability, unless other factors like beam jitter or cavity length fluctuations are present. As already remarked the SM equation (7) is appropriate for the description of the laser evolution around the maximum of the electron current, which is the center of the optical packet. On the other side, in view of the fact that the radiation explores only a small portion of the electron bunch during its passage inside the undulator, other SM-like structure may develop if sufficient gain is available around different regions of the electron packet. They are ruled by equations analogous to those given in (7), apart from a gain modulation determined by the current profile. If we sample the electron bunch with the number of peaks "predicted" by eq. (6), we obtain (numerically) what has been described in the previous parts of the paper, namely the formation of narrow subpeaks, which agrees (at least in number) with the fluctuating spikes of the SASE regime. It should also be noted that they have a spatial width of the same order of the coherence length. This is what we have found numerically using Prometeo code and an attempt of theoretical justification is provided in the Appendix.

The previous description is certainly not sufficient to explain the formation of the deep saturated comb like structure in oscillators and further remarks are in order, mainly in connection with the packet shortening. As in conventional laser devices saturation is driven by a decrease of the gain due to the intra-cavity intensity through a factor of the type

$$\begin{aligned} G(T) &\propto \frac{G}{1 + \alpha I}, \\ I &\propto |A|^2 \end{aligned} \tag{8}$$

Furthermore, since the pulse is travelling in a medium, the Kerr effect [9] produces a change of the refractive index with the intensity, namely

$$n \cong n_0 + n_2 I \tag{9}$$

where n_0, n_2 are the linear and the second order non-linear refractive indices characterizing the FEL medium. This effect produces a shift in the instantaneous phase of the pulse which in turns determines a frequency shift, leading to a frequency chirping inducing a compression of the pulse.

The mechanism is slightly more complex than the effect on single pulses propagating in selfoc fibers due to the appearance of multiple peaks, which is simply due to the finite size of

the coherence length, which, in the case of our simulations, is much shorter than the electron bunch length. An insightful analysis on this point can also be found in [12].

This is just a qualitative statement, a more detailed study in analytical terms will be presented elsewhere. A further idea of the sub-peak evolution is provided by Fig. 9 where we have reported the Nyquist diagram of a pair of different peaks. The plots provide the round trip evolution of the complex vector associated with the relevant field amplitude. We have chosen the case of the spikes 6 and 7.

In fig. 10a) we have reported the cosine of the phase difference of peaks 6 and 7 vs. the round trip number, for rt larger than 200 when the comb structure is being evidenced. The phase difference in this region is reasonably constant for a large value of rt and the peaks can reasonably be considered phase locked. In Fig. 10b) we have taken distant spikes (1-10) and the phase locking condition is reached in longer times.

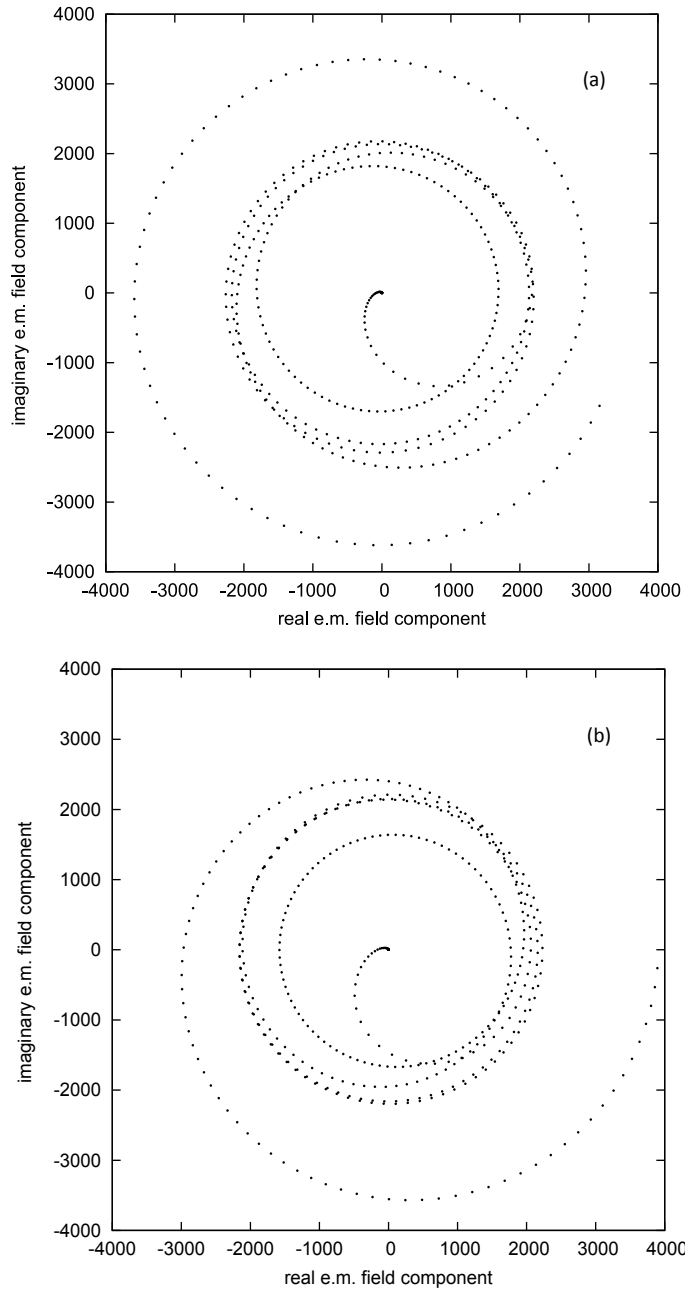


Figure 9: Round trip evolution of the real (abscissa) and imaginary (ordinate) parts of the fields in correspondence of the maximum of the sub peaks in Fig.3: a) peak 7; b) peak 6. (It is to be noted that peak 7 approaches a stationary configuration).

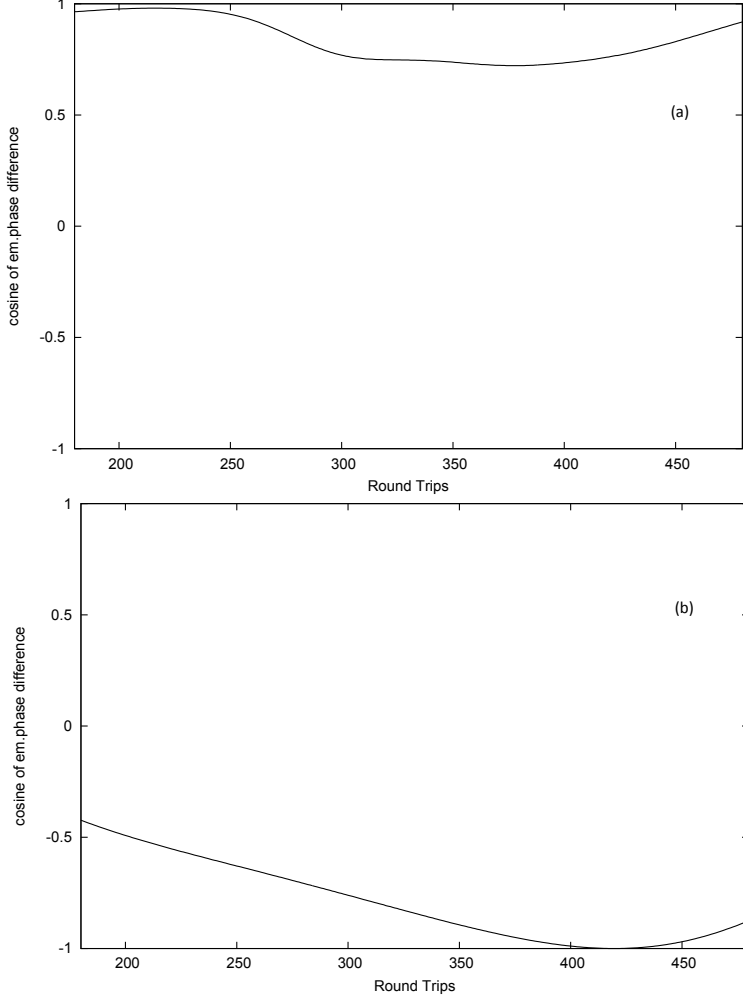


Figure 10: Round trip evolution of the cosine of the phase difference of the spikes 6 and 7 (a) and the spikes 1 and 10 (b)

We have stressed that the peak occurs at zero detuning, when the cavity is differently settled the formation of the peaks is strongly reduced. We have run the code for different values of the detuning and verified the absence of spikes deep saturated comb-like structures for $\theta \neq 0$.

A final point we want to stress is the comparison of the present result with a full 3-D code, to this aim we have modified GENESIS to run it in the oscillator mode. In Fig. 11 we have reported the field distribution at different round trip, along with the relevant spectra. The pattern of the peak formation is qualitatively similar to the dynamics predicted by the 1-D dynamics. We finally stress the content of Fig. 12, reporting the spectrum distribution at a very large round trip number ($r = 800$): the result is impressive, the spectral structure

is that of a SASE run, the only (and significant) difference is that the structure is stationary, namely it is self-reproducing after each round trip.

In this paper we have touched, with some detail, the mechanism of “spiking mode locking” in deeply saturated oscillators. Most of our considerations and results find echo in previous research [12] where the problem of the production of stable attosecond pulses has been discussed in depth. We want however to make a further remark on the results of the paper which can be summarized as the possibility of observing a comb structure in the laser pulses and on the relevant feedback on the non linear harmonic generation. The possibility of observing these effects are associated with the use of accelerating devices using e-beam with long macropulses (like Super conducting Linacs) and on the use of smooth outcoupling magnet allowing the injection of the e-beam in the second undulator [13]. In this case particular care should be devoted to design the magnets to avoid coherent synchrotron radiation emission, which might prevent the generation of higher order harmonics with the associated comb structure. A more detailed discussion will be presented in a forthcoming investigation, in which we will discuss how these effects can be implemented on the IRIDE-FEL architecture [14].

In a forthcoming investigation we will derive the mode locked slice structure by the use of a theory based on the extension of the technique of passive mode locking of conventional laser physics.

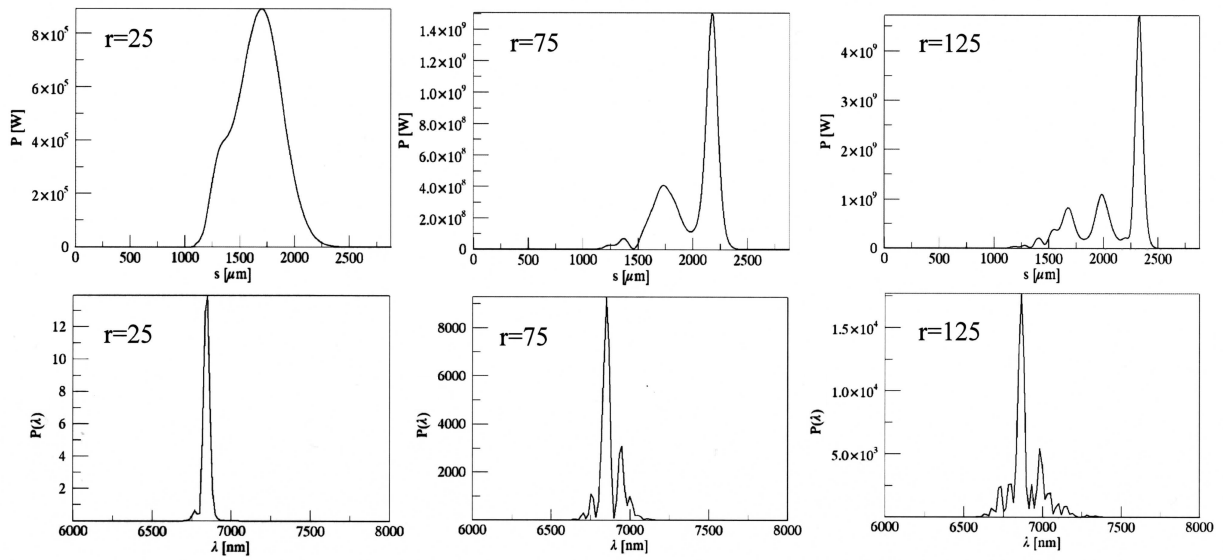


Figure 11: First line: pulse power vs position s for different values of trip number r . Second line: Spectral Intensity vs wavelength. Simulations by GENESIS 1.3.

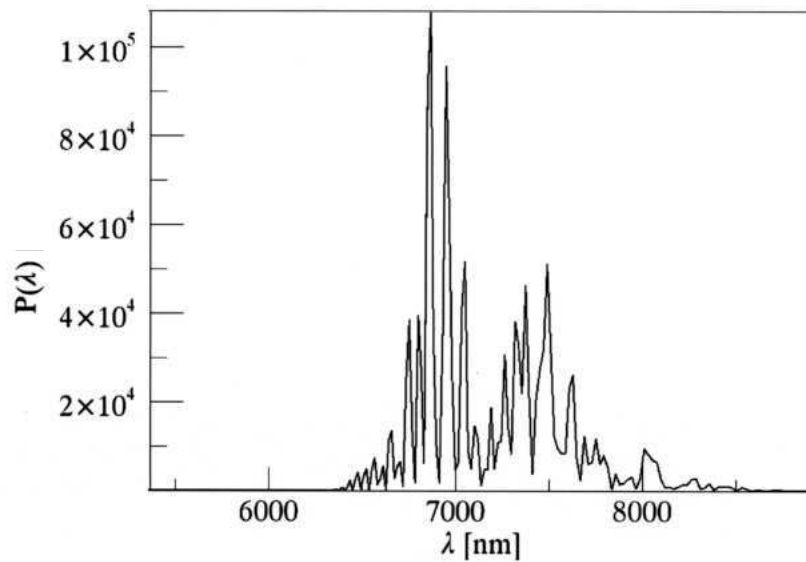


Figure 12: Spectral intensity vs wavelength at $r=800$. Simulations by GENESIS 1.3.

Appendix

In this Appendix we will discuss more quantitatively some points previously touched in qualitative terms only.

We will first clarify how the coupling parameter μ_c emerges quite naturally in the analysis of FEL gain. We assume that the electron bunch exhibits the Gaussian longitudinal distribution

$$f(z) = \frac{1}{\sqrt{2\pi\sigma_z}} e^{-\frac{z^2}{2\sigma_z^2}} \quad (10)$$

The relevant Fourier Transform (FT) writes

$$\tilde{f}(k) = \frac{1}{2\pi\sigma_z} \int_{-\infty}^{\infty} e^{-i(k-k_s)z} e^{-\frac{z^2}{2\sigma_z^2}} dz. \quad (11)$$

We have denoted by k the wave vector of a longitudinal mode. The role of the bunch distribution is that of filtering the longitudinal modes around the resonant frequency ($\omega_s = ck_s$). Using therefore as reference parameter the frequency detuning

$$\nu = 2\pi N \frac{k - k_s}{k_s} = 2\pi N \frac{\omega_s - \omega}{\omega_s} \quad (12)$$

we can write the FT in the form

$$\tilde{f}(\nu) = \frac{1}{2\pi\sigma_z} \int_{-\infty}^{\infty} e^{-i\frac{\nu}{N} \frac{z}{k_s}} e^{-\frac{z^2}{2\sigma_z^2}} dz = \frac{1}{\sqrt{2\pi}} e^{-\frac{\nu^2}{2\mu_c^2}} \quad (13)$$

The effective FEL gain accounting for the longitudinal distribution of the current is accordingly obtained by a convolution of the ordinary gain function on the distribution function (13).

The FEL gain itself is obtained by making a convolution on the gain bandwidth with the electron distribution, things should however been done by including also the effect of the slippage. The small signal field amplitude evolution in one undulator passage can be written as

$$\frac{d}{dt} a = i\pi\sqrt{2\pi}g_0 f(z + \Delta \cdot \bar{t}) \left[\int_0^{\bar{t}} d\bar{t}' (\bar{t} - \bar{t}') e^{-i\nu(\bar{t} - \bar{t}')} a(z + \Delta \cdot \bar{t}', \bar{t}') \right], \quad (14)$$

$$\bar{t} = \frac{z}{L_u}, \quad L_u \equiv \text{undulator length}$$

After expanding either the current and the field up to the second order in the slippage parameter Δ we obtain the (small signal) pulse propagation equation valid for $\Delta \ll \sigma_z$ [11]. The master FEL equation provided by eq. (7) is obtained from (14) after performing the low gain approximation $a(\bar{t}') \cong a(\bar{t})$ and iterating the single pass solution to an arbitrary

number of round trips in an optical cavity, the gain equations appearing in the master equations are just given by

$$\begin{aligned} G_2 &\propto i\partial_\nu G_1 \\ G_3 &\propto -\partial_\nu^2 G_1 \end{aligned} \quad (15)$$

And G_1 is the complex gain function [2]

$$G_1 = \frac{\pi}{\nu^3} [2(1 - e^{-i\nu\tau}) - i\nu\tau(e^{-i\nu\tau} + 1)]. \quad (16)$$

We have denoted in eq. (7) the field amplitude by “ A ” and not by “ a ” to stress the difference between the single pass and oscillator master equation. Most of this procedure and the relevant link with conventional laser Physics [9] has been discussed in [11].

Note that we have

$$\begin{aligned} A_n(\tau, T) &= \alpha_n(\tau) e^{\lambda_n \frac{T}{T_R}}, \\ \alpha_n(\tau) &\propto \frac{1}{\sqrt{2^n \sqrt{\pi} \tau_0}} H_n\left(\frac{\tau}{\tau_0}\right) e^{-\frac{\tau^2}{2\tau_0^2}}, \\ \tau_0 &\cong \frac{1}{2}\sqrt{\mu_c}, \quad \lambda_n \cong G_M - \eta - \frac{2}{3}\mu_c\left(n + \frac{1}{2}\right) \end{aligned} \quad (17)$$

(G_M =maximum small signal gain).

Using non normalized variables we find for the width of the SM

$$\sigma_b = \sigma_z \tau_0 \cong \frac{1}{2} \sqrt{\Delta\sigma_z}. \quad (18)$$

It is evident that the lowest order eigenmode ($n = 0$) is that with largest gain.

The use of the FEL gain saturation formulae yields

$$\begin{aligned} \lambda_n &\cong G_M(I_n) - \eta - \frac{2}{3}g_0\mu_c\left(n + \frac{1}{2}\right) \\ G(I_n) &= G_M \frac{1 - e^{-\beta X_n}}{\beta X_n}, \quad \beta = 1.0145 \cdot \frac{\pi}{2}, \quad X_n = \frac{I_n}{I_s} \end{aligned} \quad (19)$$

Where the saturation intensity I_s has been assumed to be the same for all the Super Modes.

The intracavity equilibrium power for $\eta \ll 1$, can be evaluated as (we refer to the fundamental SM)

$$I_e \cong (\sqrt{2} + 1) \left(\sqrt{\frac{G_M}{\eta}} - 1 \right) I_s \quad (20)$$

The pendulum equation written in normalized variables writes

$$\begin{aligned}\frac{d^2}{dt^2}\varsigma &= |a| \cos(\varsigma + \phi), \\ |a|^2 &\cong 8\pi^2 \frac{I}{I_s}\end{aligned}\tag{21}$$

thus getting, at equilibrium

$$|a| \cong \sqrt{(\sqrt{2} + 1)} 8\pi^2 \sqrt{\frac{1}{\sqrt{\frac{G_M}{\eta}} - 1}} \cong 13.8 \sqrt[4]{\frac{\eta}{G_M}}\tag{22}$$

At saturation the side band instability develops and the associated spikes correspond to half rotation of the electrons in the phase space, the necessary time for this cycle is ²

$$\Delta T \cong \frac{L_u}{2\sqrt{2}c} \sqrt{\frac{I_s}{I}}\tag{23}$$

and, at equilibrium, we find

$$\Delta T \cong \frac{L_u}{4.4c} \sqrt[4]{\frac{\eta}{G_M}}\tag{24}$$

The length of the coherent optical pulse associated with the side band instability spike, could be inferred from the slippage length occurring in one spiking cycle, namely

$$\sigma \cong \frac{N\lambda}{4.4} \sqrt[4]{\frac{\eta}{G_M}}\tag{25}$$

which, using the identity

$$N \cong \frac{(\pi g_0)^{\frac{1}{3}}}{4\pi\rho}\tag{26}$$

yields

$$\sigma \cong l_g \sqrt{3} \frac{(\pi g_0)^{\frac{1}{3}}}{4.4} \sqrt[4]{\frac{\eta}{G_M}}\tag{27}$$

For all the reasonable values of a FEL oscillator we obtain

$$\sqrt{3} \frac{(\pi g_0)^{\frac{1}{3}}}{4.4} \sqrt[4]{\frac{\eta}{G_M}} \cong 1,\tag{28}$$

the width of the side band spikes is therefore of the same order of the coherence length.

² This argument has been suggested by an anonymous Referee.

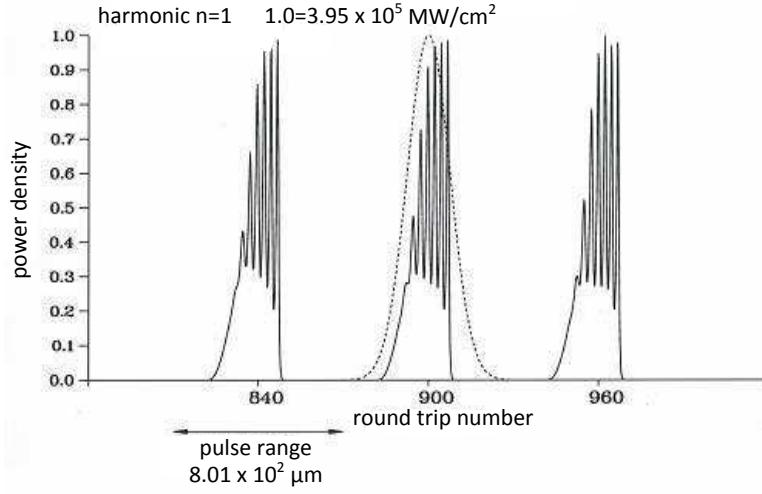


Figure 13: FEL saturated pulses at different round trips, same parameters of Fig. 2.

We have considered the dependence of the widths of the comb peaks on the cavity losses (see Fig. 13) and on the small signal gain coefficient value. The plot are the result of a simulation relevant $g_0 \cong 0.3$ and losses $\eta \cong 0.03$ accordingly we obtain a number of spikes ($n_s = 6$) consistent with eq. (6) and with a width comparable with l_c . We have tried different combinations of the parameters (gain losses, bunch length...) and the scaling relations we have hypothesized have been confirmed, along with the fact that the dependence of the sub pulse width on the cavity losses is weak.

It is evident that the previous considerations do not corroborate the suggestions that the saturated comb-spike are associated with high gain spikes, but provide a further independent argument that their duration coincides with the coherence length.

We want further to stress that when saturation has occurred around the maximum of optical packet, other regions may contribute to the growth of the field itself and should be distributed according to the “normal modes” associated with the oscillator FEL dynamics, Super Modes provide one of these possible sets. We have therefore assumed that the comb structure we have obtained in our numerical runs can be obtained as

$$S(z) \propto \alpha_{n_s}(z) e^{-\frac{z^2}{2\sigma_z^2}} \quad (29)$$

$$\alpha_{n_s} \cong \frac{1}{\sqrt{2^{n_s} \sqrt{\pi} l_c}} H_{n_s} \left(\frac{z}{l_c} \right) e^{-\frac{z^2}{2l_c^2}}$$

which is essentially the electron bunch distribution modulated with the Hermite Gauss

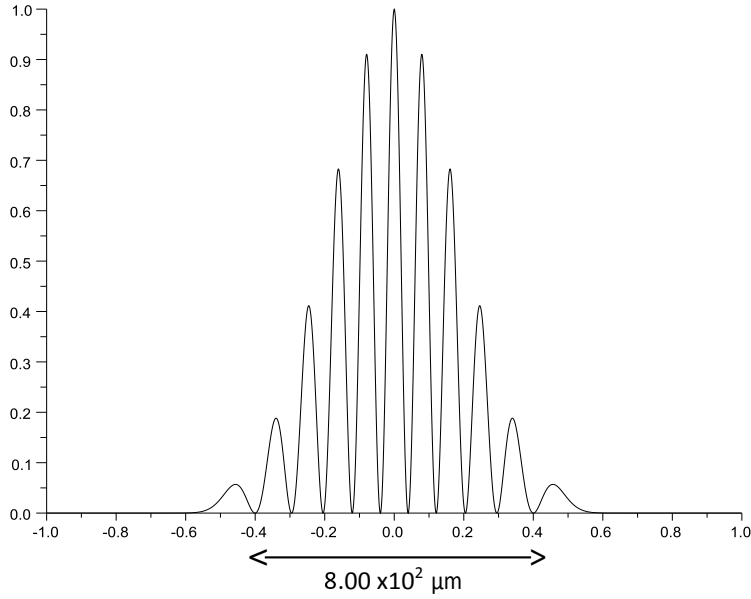


Figure 14: Comb structure (eq. (29)) to be compared with Fig.3

Super Mode basis given in eq. (15). In Fig.14 we have reported the comb structure $S(z)$ (eq. (29)) and it results that the agreement between eq. (29) and the numerical results is more than reasonable.

-
- [1] W. B. Colson, Tutorial on classical Free Electron Laser Theory, Nuclear Instruments and Methods in Physics Research A23 (1985) 1-9 North-Holland, Amsterdam.
 - [2] G. Dattoli, A. Renieri and A. Torre, Lectures on Free Electron Laser Theory and Related Topics, World Scientific, Singapore (1990).
 - [3] G. Dattoli, P. L. Ottaviani and S. Pagnutti, Booklet for FEL Design: a collection of practical formulae, ENEA RT/2007/40/FIM, G. Dattoli, P. L. Ottaviani and S. Pagnutti, J. Appl. Phys. 101(10):103109-103109-6 (2007).
 - [4] N. Nishimori, R. Hajima, R. Nagai, E.J. Minehara, Phys. Rev. Lett. 86, 5707 (2001).
 - [5] D. Nguyen, S. Russel and N. Moody, US Particle Accelerator School 2009, University of New Mexico - Albuquerque NM. The formation of these side bands has been observed in many FEL experiments, for earlier work see: R.W.Warren &al., Nucl. Instr. and Meth. A 285,1 (1989).

- [6] R. Bonifacio, C. Pellegrini and L. Narducci, *Opt. Comm.* 50, 373 (1984); E. Saldin, E. A. Schneidmiller, M.V. Yurkov, *The Physics of Free Electron Lasers*, Heidelberg, New York Springer (2000).
- [7] R. Hajima, N. Nishimori, R. Nagai and E. J. Minehara., *Nucl. Instr. Meth. A* 483, 113-118 (2002).
- [8] G. Dattoli and A. Renieri, *Il Nuovo Cimento* 61 B, 153 (1981).
- [9] Franz X. Kaertner, *Ultrafast Optics* <http://ocw.mit.edu/courses/electrical-engineering-and-computer-science/6>
H. A. Haus, *IEEE JQE* 11, 323 (1975).
- [10] P. Elleaume, *IEEE J. Quant. Elect.* QE-17 1012 (1981).
- [11] G. Dattoli, M. Del Franco, M. Labat, P. L. Ottaviani and S. Pagnutti (2012). *Introduction to the Physics of Free Electron Laser and Comparison with Conventional Laser Sources*, *Free Electron Lasers*, Dr. Sandor Varro (Ed.), ISBN: 978-953-51-0279-3, InTech, DOI: 10.5772/35429. Available from: <http://www.intechopen.com/books/free-electron-lasers/free-electron-laser-devices-a-comparison-with-ordinary>.
- [12] R. Hajima and R. Nagai, *Phys. Rev. Lett.* 91, 024801 (2003).
- [13] G.N. Kulipanov et al., *Nucl. Instr. Meth. A* 375, 576-579 (1996), A.N. Matveenko et al., *Nucl. Instr. Meth. A* 603, 38-41 (2009).
- [14] M. Ferrario et al., *Nucl. Instr. Meth. A* 740, 138-146 (2014).